

Destroying synchrony in an array of the FitzHugh–Nagumo oscillators by external DC voltage source

Elena Adomaitienė^a, Skaidra Bumelienė^a, Gytis Mykolaitis^{a,b},
Arūnas Tamaševičius^a

^aCenter for Physical Sciences and Technology,
Saulėtekio ave. 3, LT-10257 Vilnius, Lithuania
elena.tamaseviciute@ftmc.lt

^bDepartment of Physics, Vilnius Gediminas Technical University,
Saulėtekio ave. 11, LT-10223 Vilnius, Lithuania

Received: October 27, 2018 / **Revised:** July 22, 2019 / **Published online:** January 10, 2020

Abstract. A control method for desynchronizing an array of mean-field coupled FitzHugh–Nagumo-type oscillators is described. The technique is based on applying an adjustable DC voltage source to the coupling node. Both, numerical solution of corresponding nonlinear differential equations and hardware experiments with a nonlinear electrical circuit have been performed.

Keywords: coupled oscillators, FitzHugh–Nagumo oscillators, synchronization.

1 Introduction

Synchronization is widely observed in natural and artificial coupled systems, ranging from pendulum clocks to electronic, laser systems and various biological populations [6]. In most cases, e.g., radio communication, laser power systems, synchrony is a desirable state. However, sometimes it has an unfavourable impact. Synchronization of neurons in human brain is an example. It is believed that strong synchrony of spiking neurons can cause the symptoms of the Parkinson's disease and essential tremor [13]. Therefore, methods for controlling, more specifically for suppressing synchrony of coupled oscillators, particularly with possible application to neuronal arrays, are required.

A number of feedback methods for destroying synchrony in arrays of oscillators by means of feedback methods have been suggested, see, for example, [7, 9, 11, 13–15, 18, 19]. They employ either a time-delay unit [13] or a passive oscillator [19] inserted in the feedback loop. Other feedback methods use repulsive coupling [15, 18], a setup with separate registration and stimulation units [9], mean field nullifying [14, 15], and act-and-wait [11] algorithms.

The conventional, clinically approved therapy to avoid symptoms of the Parkinson’s disease is the so-called deep brain stimulation (DBS). During the DBS treatment, external periodic pulses are applied to certain brain areas [3]. The repetition rate of the pulses is usually set at about 150 Hz. In general, it should be much higher than the natural frequency of the spiking neural cells, for example, 10 Hz. The mechanism of the DBS is not fully understood. There are several papers considering the Hodgkin–Huxley and the FitzHugh–Nagumo (FHN) models and demonstrating that high frequency forcing stabilizes the unstable equilibrium of the neuronal oscillators and thus inhibit spiking cells [2, 8, 10]. Though the low frequency spikes disappear the high frequency artefact oscillations manifest. The stabilization is achieved only on the average taken over the external drive period. Moreover, due to the rectification effect in the nonlinear asymmetric oscillators, the equilibrium points are significantly shifted from their natural positions [2]. This can be the reason of the side effects often observed using the DBS.

A straightforward way to suppress the spikes is to fully stabilize the unstable steady states of the oscillators, for example, by the low-pass filter technique [1]. However, in this method, the control parameter k plays the role of both the coupling parameter and the feedback gain. To achieve stabilization, the feedback should be strong enough, i.e., above some threshold value, $k > k_{th}$. For example, in the FHN-type system investigated in [1], $k_{th} \approx 3$. In many simple control problems dealing with artificial dynamical systems, the gain k can be easily tuned to set the sufficient value. In other words, k is an adjustable parameter of the controller. However, in natural systems, like neuronal arrays, k is an intrinsic parameter of the dynamical system under control. It is not easy to vary, and in general, its value is unknown.

In this paper, we describe a simple feedback method for desynchronizing an array of the FHN oscillators not sensitive to the value of the parameter k .

2 Arrays of coupled oscillators

The corresponding circuit diagrams are presented in Fig. 1. CN is a coupling node. If the CN is not accessible directly from the outside, but via some passive resistance, a negative compensating resistor (implemented by means of a negative impedance converter) should be used, similarly as described in [14, 15].

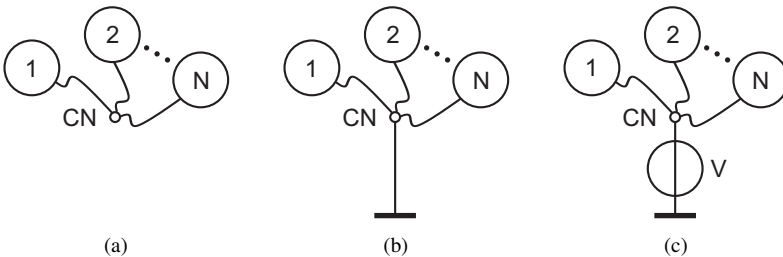


Figure 1. Arrays of mean-field coupled FHN oscillators: (a) uncontrolled, (b) the mean-field nullifying technique, (c) the DC voltage source technique.

3 Mathematical model

An individual FHN oscillator is given by [16]

$$\begin{aligned} \dot{x} &= ax - f(x) - y - c, \\ \dot{y} &= x - by. \end{aligned} \tag{1}$$

Variable x represents the membrane potential, variable y describes the recovery process, $ax - f(x)$ is the activation function, b is the damping parameter, $f(x)$ is a nonlinear function presented by a three-segment piecewise linear function

$$f(x) = \begin{cases} d(x + 1), & x < -1, \\ 0, & -1 \leq x \leq 1, \\ g(x - 1), & x > 1. \end{cases} \tag{2}$$

For $d \gg g$ [16], the $f(x)$ is an essentially asymmetric function in contrast to the common FHN cubic parabola x^3 introduced by FitzHugh [5]. The steady state is

$$x_0 = -\frac{bc}{1-ab}, \quad y_0 = -\frac{c}{1-ab}. \tag{3}$$

Expressions (3) are valid for $ab < 1$ and relatively small product $|c|b$ ($|c|b \leq 1 - ab$), that is, for $-1 \leq x_0 \leq 1$ when according to formula (2), $f(x_0) = 0$. Equations (1) linearised around the steady state read:

$$\dot{x} = ax - y, \quad \dot{y} = x - by. \tag{4}$$

Equations (4) can be presented in the following form:

$$\ddot{x} - (a - b)\dot{x} + (1 - ab)x = 0.$$

The corresponding characteristic equation is

$$\lambda^2 - (a - b)\lambda + 1 - ab = 0.$$

Its solutions are

$$\lambda_{1,2} = \frac{a - b}{2} \pm \sqrt{\frac{(a - b)^2}{4} - 1 + ab} = \frac{a - b}{2} \pm \sqrt{(a + b)^2 - 4}. \tag{5}$$

If $a > b$, then the real parts of λ are positive, and the steady state (3) is unstable.

An array of N isolated oscillators is given by

$$\begin{aligned} \dot{x}_i &= ax_i - f(x_i) - y_i - c_i, \\ \dot{y}_i &= x_i - by_i, \quad i = 1, 2, \dots, N. \end{aligned}$$

Here the bias parameters c_i are intentionally set different for each individual oscillator, thus making them nonidentical units. The parameters a and b , as well as the nonlinear

function $f(\cdot)$, are the same for all oscillators. Similarly to the single oscillator given by Eqs. (1), that is, assuming $ab < 1$ and $|c_i|b \leq 1 - ab$, the steady states are

$$x_{0i} = -\frac{bc_i}{1-ab}, \quad y_{0i} = -\frac{c_i}{1-ab}, \quad i = 1, 2, \dots, N.$$

Performing the same stability analysis as for the single oscillator, we find that all steady states (x_{0i}, y_{0i}) in the array are unstable if $a > b$ (the real parts of all eigenvalues λ_i of the corresponding characteristic equations are positive). If, in addition to $a > b$, the sum $a + b > 2$ (as in the numerical simulations presented in Section 4), then all eigenvalues are real (do not have imaginary parts). Thus, the steady states are unstable nodes.

An array of mean-field coupled oscillators (Fig. 1(a)) is given by

$$\begin{aligned} \dot{x}_i &= ax_i - f(x_i) - y_i - c_i + k(x_m - x_i), \\ \dot{y}_i &= x_i - by_i, \quad i = 1, 2, \dots, N. \end{aligned} \quad (6)$$

Here k is the coupling parameter; for simplicity, it is assumed to be the same for all oscillators. x_m is the mean of all variables x_i :

$$x_m(t) = \frac{1}{N} \sum_{i=1}^N x_i(t).$$

The mean variable $x_m(t)$ in Eqs. (6), provided $k \neq 0$, is the reason of synchronization of the oscillators.

An array controlled using the mean-field nullifying technique (Fig. 1(b)) is described by

$$\begin{aligned} \dot{x}_i &= ax_i - f(x_i) - y_i - c_i + k(0 - x_i), \\ \dot{y}_i &= x_i - by_i, \quad i = 1, 2, \dots, N. \end{aligned}$$

Here, in comparison with Eqs. (6), the mean field x_m is intentionally set zero, that is, the reason causing synchronization is straightforwardly removed.

An array controlled using an external DC voltage (Fig. 1(c)) is given by

$$\begin{aligned} \dot{x}_i &= ax_i - f(x_i) - y_i - c_i + k(v - x_i), \\ \dot{y}_i &= x_i - by_i, \quad i = 1, 2, \dots, N. \end{aligned} \quad (7)$$

Here v is a constant (adjustable) parameter representing the external DC voltage source. Evidently, the mean-field nullifying method, described in [14, 15], is a special case of the external DC voltage technique with $v = 0$. Since $v = \text{const}$, i.e., v does not vary with time and does not depend on variables x_i , the coupling is effectively removed, and synchronization is destroyed.

Analysis of the $2N$ -dimensional coupled system (6) is very complicated. It can be simplified using the mean-field approach. The mean-field variables are obtained by direct averaging the all terms in Eqs. (6):

$$\begin{aligned} \dot{x}_m &= ax_m - f_m(x_i) - y_m - c_m, \\ \dot{y}_m &= x_m - by_m. \end{aligned} \quad (8)$$

Here

$$\begin{aligned}
 x_m &= \frac{1}{N} \sum_{i=1}^N x_i, & y_m &= \frac{1}{N} \sum_{i=1}^N y_i, \\
 c_m &= \frac{1}{N} \sum_{i=1}^N c_i, & f_m(x_i) &= \frac{1}{N} \sum_{i=1}^N f(x_i).
 \end{aligned}$$

Note that Eqs. (8) lack the coupling term $k(\cdot)$. It is nullified for all k since $k(x_m - x_i)_m = k(x_m - x_m) = 0$. Equations (8) cannot be used to describe the dynamics of the mean field because the function $f_m(x_i) \neq f(x_m)$. However, it can be employed to derive the mean steady state. If, for all i , $|c_i|b \leq 1 - ab$, then $-1 \leq x_{0i} \leq 1$. According to definition of the nonlinear function $f(x)$, $f(-1 \leq x_{0i} \leq 1) = 0$ and, consequently, $f_m(x_{0i}) = 0$. Eventually, the steady state of the mean field is obtained:

$$x_{0m} = -\frac{bc_m}{1 - ab}, \quad y_{0m} = -\frac{c_m}{1 - ab}. \tag{9}$$

Stability analysis shows that the mean steady state (9) is unstable for $a > b$, similarly to the case the single oscillators.

The steady states of the controlled system can be easily derived from Eqs. (7) because it is an effectively decoupled system

$$x_{0i} = -\frac{b(c_i - kv)}{1 - (a - k)b}, \quad y_{0i} = -\frac{c_i - kv}{1 - (a - k)b}, \quad i = 1, 2, \dots, N. \tag{10}$$

Equations (7) linearised around the steady states (10) read:

$$\begin{aligned}
 \dot{x}_i &= (a - k)x_i - y_i, \\
 \dot{y}_i &= x_i - by_i, \quad i = 1, 2, \dots, N.
 \end{aligned}$$

The corresponding characteristic equations are

$$\lambda_i^2 - (a - b - k)\lambda_i + 1 - (a - k)b = 0, \quad i = 1, 2, \dots, N.$$

The eigenvalues λ_i do not depend on i and are similar to the case of the single oscillator (5), except the coupling parameter k :

$$\lambda_{1,2} = \frac{a - b - k}{2} \pm \sqrt{\frac{(a - b - k)^2}{4} - 1 + (a - k)b}.$$

The real parts of λ are positive, and the steady sates are still unstable for $k < k_{th}$, whereas the real parts become negative, and the steady states become stabilized for $k > k_{th}$, where $k_{th} = a - b$.

4 Numerical results

Typical waveforms for synchronized and desynchronized FHN oscillators are presented in Fig. 2. Synchronized oscillators (Fig. 2(a)) all oscillate at the same frequency with a constant phase shift. The amplitude of mean variable x_m is high, whereas desynchronized oscillators (Fig. 2(b)) exhibit different frequencies and low amplitude of the mean variable x_m . Waveforms in Fig. 2 are shown for relatively small coupling parameter ($k = 0.4 < k_{th}$), which ensures that, for all oscillators given by Eqs. (6) and Eq. (7), the steady states are unstable.

Results for other values of k are summarized in Fig. 3. We characterize the oscillations by the root mean square (RMS) of the $x_m - \langle x_m \rangle$:

$$\text{RMS} = \sqrt{\langle (x_m - \langle x_m \rangle)^2 \rangle} = \sqrt{\langle x_m^2 \rangle - \langle x_m \rangle^2}.$$

Here and elsewhere the angle brackets $\langle \cdot \rangle$ represent averaging over time. At $k = 0$, the RMS calculated from Eq. (6) and from Eq. (7) coincide, as expected. The RMS becomes high at $k \geq 0.4$ in the case synchronized oscillators. It slowly diminishes for desynchronized oscillators. Eventually, RMS drops to zero at $k > k_{th} = 3.24$. At this point quite different mechanism, namely stabilization of the steady state, starts to play the role. Oscillations are fully damped, yielding $\text{RMS} = 0$. The average $\langle x_m \rangle$ in Fig. 3 saturates to -0.43 , which coincides with the value of x_{0m} calculated either directly from formula (9) or from formula (10) using the appropriate parameter values: $a = 3.4$, $b = 0.16$, $c_m = 1.24$, $k = k_{th} = 3.24$, $v = -0.43$. Formally, the adjustable

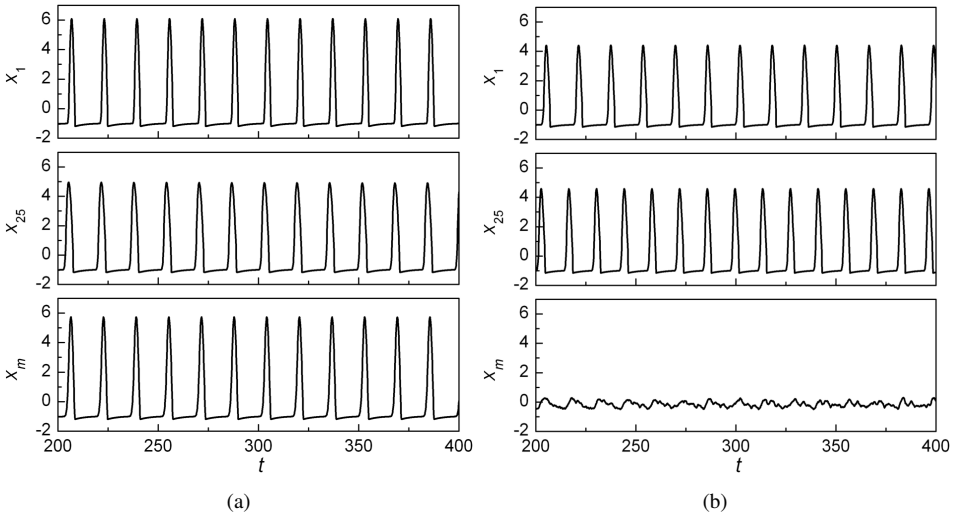


Figure 2. Waveforms $x_1(t)$, $x_{25}(t)$, and $x_m(t)$: (a) synchronized oscillators from Eq. (6), (b) desynchronized oscillators from Eq. (7). $N = 25$, $a = 3.4$, $b = 0.16$, $c_i = 44/(24 + i)$, $d = 60$, $g = 3.4$, $k = 0.4$, $v = -0.15$.

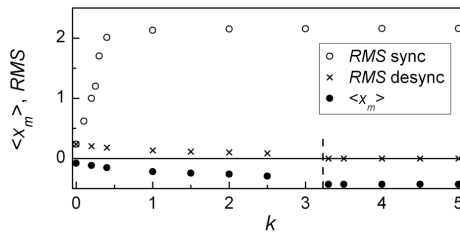


Figure 3. RMS and $\langle x_m \rangle$ vs. the parameter k . Other parameters are the same as in Fig. 2, except v adjusted for each k . Vertical dashed line indicates $k = k_{th} = 3.24$.

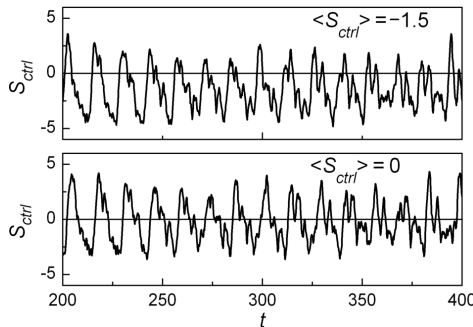


Figure 4. Full control signals in the case of desynchronized oscillators (small k). $N = 25$, $a = 3.4$, $b = 0.16$, $c_i = 44/(24 + i)$, $d = 60$, $g = 3.4$, $k = 0.4$. Top: mean field nullifying technique ($v = 0$), $S_{ctrl} = kNx_m$. Bottom: DC voltage source technique ($v \neq 0$), $S_{ctrl} = kN(x_m - v)$, $v = -0.15$.

parameter v in Eq. (7) can be freely selected. Desynchronization is always achieved (even for $v = 0$ [15]). The constant parameter v (independent on variables x_i) replaces the variable x_m in Eqs. (6), i.e., it removes the reason of synchronization. However, improper v causes strong DC current into the system under control. This can be a harmful artefact in the case of biological systems. The total control signal is given by

$$S_{ctrl} = - \sum_{i=1}^N k(v - x_i) = kN(x_m - v).$$

The S_{ctrl} should not have DC component, i.e., its time average should be zero, $\langle S_{ctrl} \rangle = 0$. This equality serves as a criterion for the proper value of v .

Two control methods, namely the mean field nullifying technique and the DC voltage source technique are compared in Figs. 4 and 5.

For weak coupling ($k < k_{th}$), when the oscillators are desynchronized, but are still active, the control signals have similar amplitude and shape (Fig. 4), for both the mean field nullifying technique and the DC voltage source technique. However, the latter has an advantage in the sense that the time average of the control signal has no undesirable DC component, $\langle S_{ctrl} \rangle = 0$.

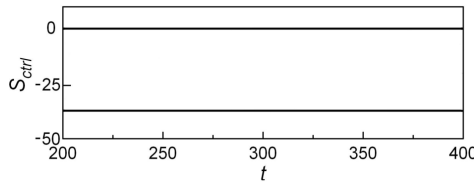


Figure 5. Full control signals in the case of stabilized steady states (large k). $N = 25$, $a = 3.4$, $b = 0.16$, $c_i = 44/(24 + i)$, $d = 60$, $g = 3.4$, $k = 3.4$. Lower line at -36.6 level is the mean field nullifying technique ($v = 0$), $S_{ctrl} = kNx_m$. Upper line at 0 level is the DC voltage source technique ($v \neq 0$), $S_{ctrl} = kN(x_m - v)$, $v = -0.43$.

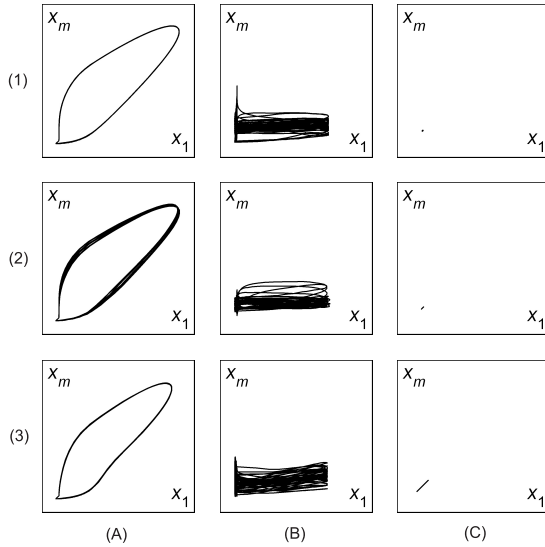


Figure 6. Phase portraits [x_m vs. x_1]. Column (A): synchronized oscillators, $k = 0.4$; Column (B): desynchronized oscillators, $k = 0.4$, $v = -0.15$; Column (C): stabilized oscillators, $k = 3.4$, $v = -0.43$. Row (1): without perturbation, $A = 0$; Row (2): low (3%) perturbation, $A = 0.1$; Row (3): moderate (15%) perturbation, $A = 0.5$. $N = 25$, $a = 3.4$, $b = 0.16$, $c_i = 44/(24 + i)$, $d = 60$, $g = 3.4$, $\omega = 2$.

Similarly, in the case of strong coupling ($k > k_{th}$), when all oscillators are totally damped (Fig. 5), the merit of the proposed method is evident. Though both methods exhibit constant (nonoscillating) control signals, the DC voltage source technique distinguishes itself by zero level (Fig. 5, upper line).

The above results are presented for an idealized case, when the environmental interference is ignored. Therefore, we performed an additional case study of the proposed method with an external perturbation. A periodical perturbation has been added to Eq. (7): $\dot{x}_i = \dots + A \sin(\omega t)$. It mimics the situation when real neurons, spiking at the rate of 10 Hz (α -rhythm), can be influenced by the environmental interference at 50 Hz (5 times higher than the α -rhythm) from the surrounding electrical devices and installation. Respectively, the parameter ω is set to ensure that the interference frequency is higher than the rate of the spikes in Fig. 2 by a factor of 5. The results are presented in Fig. 6 in the form of

the phase portraits, which are visually more sensitive to perturbations, than simple time sequences in Fig. 2. The phase portraits demonstrate that the control method is robust against moderate level of external interference (the amplitude $A = 0.5$ corresponds to about 15% of the spike amplitude). Some influence is observed for the stabilized steady states: the dot in Fig. 6(1)(C) has evolved to a fine short diagonal in Fig. 6(3)(C), typical to the nonautonomous states synchronized to the external force.

5 Electronic experiments

Single FHN oscillator is sketched in Fig. 7. OA is a general-purpose operational amplifier, e.g., NE5534-type device, D_1 and D_2 are the BAV99-type diodes, $L = 10$ mH, $C = 3.3$ nF, $R_1 = R_2 = 1$ k Ω , $R_3 = 510$ Ω , $R_4 = 30$ Ω , $R_5 = 510$ Ω (note $R_5 \gg R_4$), $R_6 = 275$ Ω (an external resistor $R'_6 = 220$ Ω in series with the coil resistance $R''_6 = 55$ Ω), $R_7^{(i)} = (24 + i)$ k Ω , $i = 1, 2, \dots, N$, $R^* = 5.1$ k Ω , $V_0 = -15$ V. In the experiments we employed a hardware array with $N = 30$, described in details (without any external control) elsewhere [17]. The experimental results are shown in Fig. 8.

The dimensionless variables and parameters in the equations (Section 3 are related to the circuit variables and element values in the following way:

$$x_i = \frac{V_{Ci}}{V^*}, \quad y_i = \frac{\rho I_{Li}}{V^*}, \quad t \rightarrow \frac{t}{\sqrt{LC}}, \quad x_m = \frac{1}{NV^*} \sum_{i=1}^N V_{Ci}, \quad \rho = \sqrt{\frac{L}{C}},$$

$$a = \frac{\rho}{R_3}, \quad b = \frac{R_6}{\rho}, \quad c_i = \frac{\rho V_0}{R_7^{(i)} V^*}, \quad d = \frac{\rho}{R_4}, \quad g = \frac{\rho}{R_5}, \quad k = \frac{\rho}{R^*}, \quad v = \frac{V}{V^*}.$$

Here V^* is the breakpoint voltage of the forward $I-V$ characteristic of the diodes ($V^* \approx 0.6$ V), V is an external adjustable DC voltage (Fig. 1(c)).

The photos in Fig. 8 have been taken from the screen of a multichannel oscilloscope. The waveforms for only two individual oscillators, namely $i = 1$ and $i = 30$ of the array and the mean variable $V_{Cm}(t)$ are presented. The waveforms for other oscillators ($i = 2, 3, \dots, 29$) have been also inspected. All experimental waveforms are similar to the simulated ones in Fig. 2. Low amplitude of $V_{Cm}(t)$ in Fig. 8(b) indicates that the oscillators are desynchronized.

The blurred waveform of $V_{C30}(t)$ in Fig. 8(b) might be somewhat puzzling and therefore needs an explanation. The point is that the oscilloscope operated not in a single-shot,

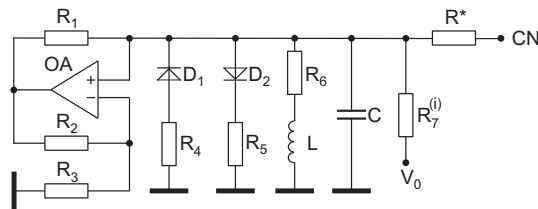


Figure 7. Circuit diagram of a single FHN oscillator. CN is the coupling node in Fig. 1. The bias resistors $R_7^{(i)}$ are set different for each oscillator, whereas the coupling resistors R^* are the same in all oscillators.

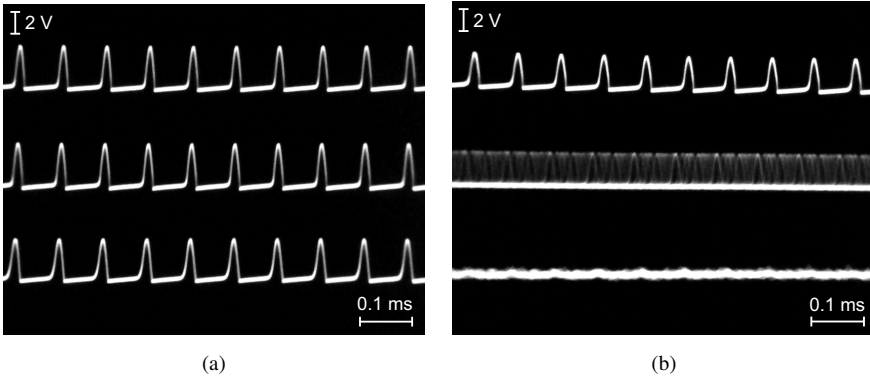


Figure 8. Waveforms: (a) synchronized oscillators, (b) desynchronized oscillators. In (a) and (b), top traces are $V_{C1}(t)$, middle traces are $V_{C30}(t)$, and bottom traces are $V_{Cm}(t)$. $V = -90$ mV ($v = -0.15$).

but in a multi-sweep mode. Synchronization of the multichannel oscilloscope was set to the first channel (the sweep generator was driven by $V_{C1}(t)$). Consequently, when the oscillators are desynchronized all signals $V_{Ci}(t)$, except the $V_{C1}(t)$, look blurred. This is another useful experimental indication of desynchronization.

Concerning the interference, considered in the numerical simulation, we note that both the intrinsic noise in the passive and the active electronic devices and the environmental interference are included automatically in the electronic experiments.

6 Concluding remarks

The proposed technique for desynchronizing arrays of the FitzHugh–Nagumo oscillators using the DC voltage source has an advantage over the earlier described mean-field nullifying technique [14, 15]. The benefit, in particular for biological systems, is that the new technique allows to avoid undesirable DC current component in the control signal. Formally, the proposed technique reminds the transcranial direct-current stimulation (tDCS, also abbreviated as tcDCS), used to treat depression [4]. Both of them employ the DC sources. However, there is an essential difference between these techniques. In the tDCS, a DC *current* is injected via the scalp to the brain. In our case, the DC *voltage* is applied to the system. Moreover, the DC voltage value is adjusted so that the current is zero.

Depending on the coupling strength of the oscillators, there are two different physical mechanisms yielding low amplitude of the mean-field variable $x_m(t)$. The first one, observed at weak coupling ($k < k_{th}$), is the desynchronization in the narrow sense. When the mean field variable x_m in the coupling terms is replaced with an external parameter v , all the individual units start to oscillate at different frequencies and phases, like in an array of isolated oscillators, thus providing low RMS. The second mechanism, manifesting at stronger coupling ($k > k_{th}$), leads to stabilization of the originally unstable steady states (x_{0i}, y_{0i}) resulting in full damping of the units, thus yielding RMS = 0. In this case, the concept of synchronization/desynchronization lacks its narrow sense (though very

formally we can consider nonoscillating units as “synchronized” to zero frequency with only some differences of their stabilized steady states). So, for any k , the RMS of the mean-field variable is either low or even zero, whereas the average of the total control signal vanishes, $\langle S_{\text{ctrl}} \rangle = 0$.

Concerning the influence of external interference, we performed simulation with an additive periodical perturbations imitating the influence of the environmental interference at 50 Hz from electrical equipment and installation. No substantial influence has been observed, at least to moderate level (15%) of perturbation.

Regarding possible practical application of the DC voltage technique to real neural systems, maybe the same electrode setup, used in the DBS treatment, can be exploited. However, in this concern, deeper research is required, since the mechanism of electrical stimulation delivery to the neurons is more complicated than in simple electrical circuits [8, 12].

References

1. E. Adomaitienė, S. Bumelienė, G. Mykolaitis, A. Tamaševičius, Stabilization of a network of the FitzHugh–Nagumo oscillators by means of a single capacitor based RC filter feedback technique, *Complexity*, **2017**:4324879, 2017.
2. E. Adomaitienė, G. Mykolaitis, S. Bumelienė, A. Tamaševičius, Inhibition of spikes in an array of coupled FitzHugh–Nagumo oscillators by external periodic forcing, *Nonlinear Anal. Model. Control*, **22**(3):421–429, 2017.
3. A. L. Benabid, S. Chabardes, J. Mitrofanis, P. Pollak, Deep brain stimulation of the subthalamic nucleus for the treatment of Parkinson’s disease, *Lancet Neurol.*, **8**(1):67–81, 2009.
4. A.R. Brunoni, A.H. Moffa, F. Fregni, U. Palm, F. Padberg, D.M. Blumberger, Z.J. Daskalakis, D. Bennabi, E. Haffen, A. Alonzo, C.K. Loo, Transcranial direct current stimulation for acute major depressive episodes: Meta-analysis of individual patient data, *Brit. J. Psychiat.*, **208**(6):522–531, 2016.
5. R. FitzHugh, Impulses and physiological states in theoretical models of nerve membrane, *Biophys. J.*, **1**(6):445–466, 1961.
6. A. Pikovsky, M. Rosenblum, J. Kurths, *Synchronization: A Universal Concept in Nonlinear Sciences*, Cambridge Univ. Press, Cambridge, 2003.
7. O.V. Popovych, C. Hauptmann, P.A. Tass, Effective desynchronization by nonlinear delayed feedback, *Phys. Rev. Lett.*, **94**:164102, 2005.
8. K. Pyragas, V. Novičenko, P.A. Tass, Mechanism of suppression sustained neuronal spiking under high-frequency stimulation, *Biol. Cybern.*, **107**:669–684, 2013.
9. K. Pyragas, O.V. Popovych, P.A. Tass, Controlling synchrony in oscillatory networks with a separate stimulation-registration setup, *Eur. Phys. Lett.*, **80**:40002, 2007.
10. K. Pyragas, P.A. Tass, Suppression of spontaneous oscillations in high-frequency stimulated neuron models, *Lith. J. Phys.*, **156**:223–238, 2016.
11. I. Ratas, K. Pyragas, Controlling synchrony in oscillatory networks via an act-and-wait algorithm, *Phys. Rev. E*, **90**:032914, 2014.

12. F. Rattay, Analysis of models for extracellular fiber stimulation, *IEEE Trans. Biomed. Eng.*, **36**(7):676–682, 1989.
13. M. G. Rosenblum, A. S. Pikovsky, Controlling synchronization in an ensemble of globally coupled oscillators, *Phys. Rev. Lett.*, **92**:114102, 2004.
14. A. Tamaševičius, G. Mykolaitis, E. Tamaševičiūtė, S. Bumelienė, Two-terminal feedback circuit for suppressing synchrony of the FitzHugh–Nagumo oscillators, *Nonlinear Dyn.*, **81**: 783–788, 2015.
15. A. Tamaševičius, E. Tamaševičiūtė, G. Mykolaitis, Feedback controller for destroying synchrony in an array of the FitzHugh–Nagumo oscillators, *Appl. Phys. Lett.*, **101**:223703, 2012.
16. A. Tamaševičius, E. Tamaševičiūtė, G. Mykolaitis, S. Bumelienė, R. Kirvaitis, R. Stoop, Neural spike suppression by adaptive control of an unknown steady state, in C. Alippi, M. Polycarpou, C. Panayiotou, G. Ellinas (Eds.), *Artificial Neural Networks – ICANN 2009*, Springer, Berlin, Heidelberg, 2009, pp. 618–627.
17. E. Tamaševičiūtė, G. Mykolaitis, A. Tamaševičius, Analogue modelling an array of the FitzHugh–Nagumo oscillators, *Nonlinear Anal. Model. Control*, **17**(1):118–125, 2012.
18. L.S. Tsimring, N.F. Rulkov, M.L. Larsen, M. Gabbay, Repulsive synchronization in an array of phase oscillators, *Phys. Rev. Lett.*, **95**:014101, 2005.
19. N. Tukhlina, M. Rosenblum, A. Pikovsky, J. Kurths, Feedback suppression of neural synchrony by vanishing stimulation, *Phys. Rev. E*, **75**:011918, 2007.